Wavelength-domain tracking in multiple-beam optical storage systems

Taeyoung Choi, MEMBER SPIE
Tom D. Milster, FELLOW SPIE
Matthew Lang
University of Arizona
Optical Sciences Center
Tucson, Arizona 85721
E-mail: tchoi@optics.arizona.edu

Abstract. Wavelength-domain tracking (WDT) is a new concept for application in multiple-beam optical storage systems. Tracking errors caused by use of multiple beams on curved tracks are avoided in WDT systems by optimizing separations of focused beam spots. The control of beam spot separations is accomplished by wavelength tuning of individual laser sources. Feasibility of WDT is demonstrated by implementation and testing of a single-beam WDT tracking servo. Also, a novel method of error signal extraction by low-frequency modulation is proposed.
[DOI: 10.1117/1.1901656]

Subject terms: wavelength-domain tracking; tracking error signal; external cavity diode laser; blazed grating; optical data storage; multiple-beam lasers.

Paper 040449 received Jul. 10, 2004; revised manuscript received Nov. 16, 2004; accepted for publication Nov. 17, 2004; published online Apr. 22, 2005.

1 Introduction

A straightforward method to increase the data rate in optical data storage systems is to use more than one laser beam in parallel. A number of methods have been implemented to achieve simultaneous recording and reading on multiple tracks. Depending on the methods of generating multiple beams, they can be divided into three categories: a diffractive optical element,[1] a diode laser array,[2] and a combination of laser diodes and a beam combiner.[3] However, these schemes have difficulty in controlling optimum beam spot spacing as a function of disk radius. Since radii of inner-diameter (ID) and outer-diameter (OD) tracks are different, multiple beams centered perfectly on inner tracks produce track errors at outer radii, unless separations of beam spots are changed. Also, track eccentricity causes tracking errors in multiple-beam systems.

The ID/OD errors are evaluated with a simple mathematical development. If an array consists of N beams with separation s between beams, the array length l is $(N-1)s$. The required beam separation is larger than the track pitch, so as to avoid thermal cross talk between adjacent beams. For example, a beam separation of $s=10\,\mu$m is reported to limit thermal cross talk below -48 dB in one system.[4] Therefore, the beam array is slanted at an angle ψ, such that the beam spots are positioned on adjacent tracks and separated sufficiently to avoid thermal cross talk. Figure 1(a) shows beam spot arrays at inner and outer tracks. Beam spot 1 is centered on an inner track at radius r_1, and beam spot 2 is located on an inner track of radius $r_2=r_1+d$, where d is the track pitch. The track radius r_N for beam spot N is given by

$$r_N=r_1+(N-1)d. \tag{1}$$

The position of beam spot N is expressed in terms of l, ψ, and r_1 as

$$x=l\sin\psi, \tag{2}$$

and

$$y=r_1+l\cos\psi. \tag{3}$$

The values of x and y should satisfy the equation for a circle of radius r_N, which is given by

$$x^2+y^2=r_N^2. \tag{4}$$

The beam array angle is calculated from substituting Eqs. (2) and (3) into Eq. (4). That is,

$$\psi=\cos^{-1}\left(\frac{r_N^2-r_1^2-l^2}{2r_1l}\right). \tag{5}$$

If the beam array is moved outwardly with the beam array angle and beam separation fixed in the radial direction so that beam spot 1 is placed at radius r_1', the position of beam spot N is given by

$$x'=l\sin\psi, \tag{6}$$

and

$$y'=r_1'+l\cos\psi. \tag{7}$$

Due to the difference in radii, beam spot N is not centered on a track. The error q_r is the difference between the radius of the desired track for beam spot N and the distance of the actual position of beam spot N from the disk center. That is,

$$q_r=|r_N'-[(x')^2+(y')^2]^{1/2}|. \tag{8}$$

Errors of beam spot N are calculated using Eq. (8) with $N=10$, $s=10\,\mu$m, $r_1=25$ mm, and $d=0.74\,\mu$m, where the track pitch of a digital versatile disk (DVD) is used in the

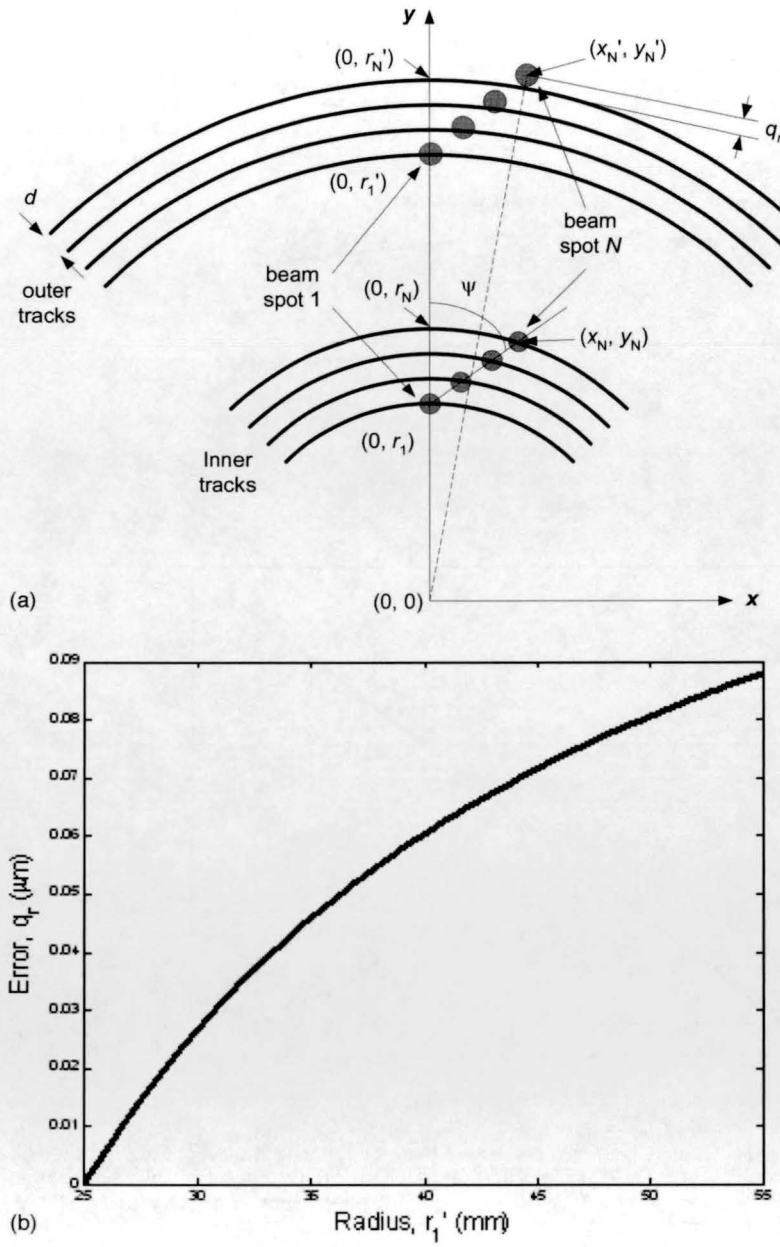

Fig. 1 Error caused by difference in radii in a multiple-beam system with a fixed spot separation. (a) Geometry of multiple beams at inner and outer tracks. (b) Estimated error q_r of beam spot N at radius r_1' with $N=10$, $s=10\ \mu$m, $r_1=25$ mm, and $d=0.74\ \mu$m.

calculation. Figure 1(b) shows the estimated error at the outer radius r_1'. The maximum error is about 0.09 μm, which is greater than one-tenth of the track pitch and is considered an unacceptable tracking error.

In addition, track runout caused by discrepancy between the actual track center and the mechanical center of rotation gives rise to track errors in multiple-beam systems with a fixed beam spot separation. Error due to track runout is estimated as follows. Beam angle ψ is set to locate multiple beam spots on separate horizontal tracks, and the observation point lies on a diameter line, as shown in Fig. 2(a). When beam spot 1 is centered on track 1, beam spot 2 is slightly off-centered from track 2 in the presence of track decenter $\Delta\epsilon$, because tracks are not perpendicular to the rotational center at the observation point. The beam array angle ψ is determined from Eq. (5). Track tilt angle δ expressed in terms of $\Delta\epsilon$ and radius r_1 is

$$\delta=\sin^{-1}\left(\frac{\Delta\epsilon}{r_1}\right). \tag{9}$$

Track error q_ϵ of two beams is the subtraction of the distance of beam spot 2 from track 1 and the track pitch. That is,

$$q_\epsilon=s\cos(\psi-\delta)-d. \tag{10}$$

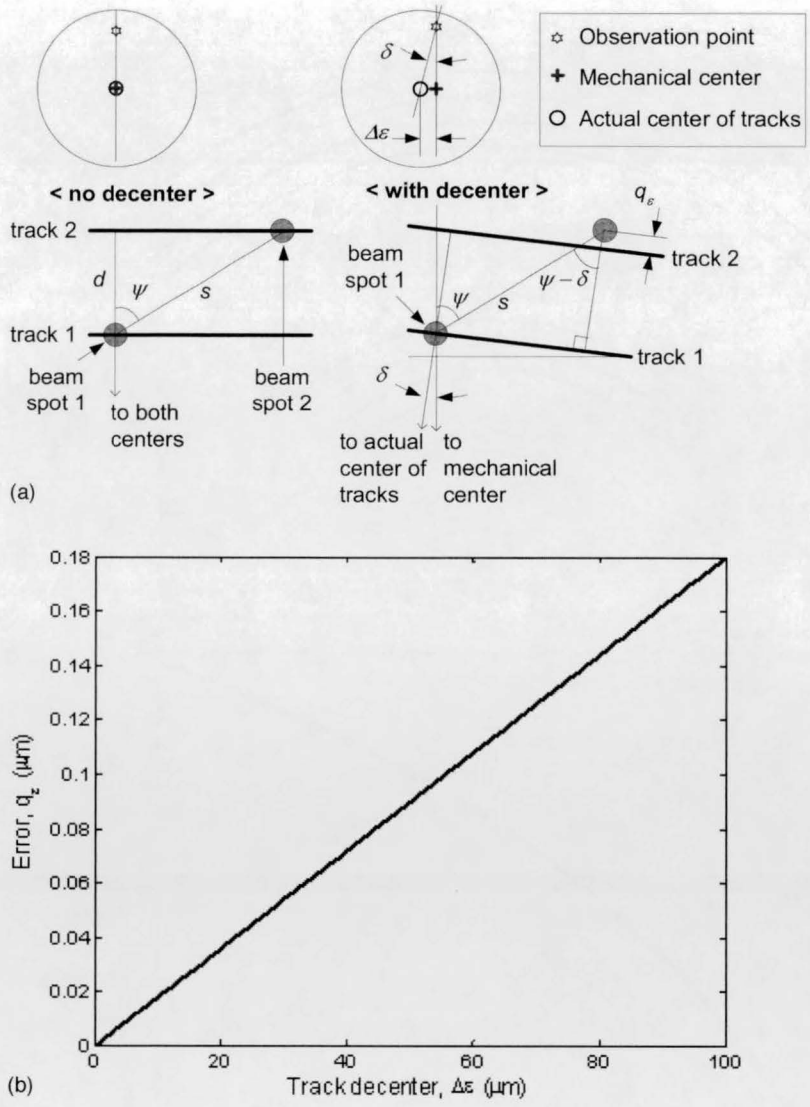

Fig. 2 Error caused by discrepancy between the actual track center and the mechanical center of rotation in a multiple-beam system with a fixed spot separation. (a) Geometry of multiple beams without and with track decenter $\Delta\epsilon$. (b) Estimated error q_ϵ of beam spot N at $\Delta\epsilon$ with $N=10$, $s=10\,\mu$m, $r_1=50$ mm, and $d=0.74\,\mu$m.

When N beams are used, track error q_ϵ is given by

$$q_\epsilon=(N-1)[s\cos(\psi-\delta)-d]. \tag{11}$$

Figure 2(b) shows q_ϵ for beam spot N due to track decenter. For $N=10$, $s=10\,\mu$m, $r_1=50$ mm, and $d=0.74\,\mu$m, a track decenter of $\Delta\epsilon=100\,\mu$m creates $q_\epsilon=0.18\,\mu$m, which, again, is greater than one-tenth of the track pitch.

The total error q_T to misalignment of the multiple beams is

$$q_T=q_r+q_\epsilon. \tag{12}$$

For the example given, q_T has a maximum value of 0.27 μm, which is well beyond a reasonable tolerance of $d/10=0.07\,\mu$m for DVD systems. Therefore, significantly degraded signal quality is expected on the outer-most beams in the array. This q_T value cannot be corrected without a complicated beam rotation or magnification adjustment scheme using conventional optical layouts. However, the required electrical bandwidth for the correction corresponds to only a one-half or one-quarter rotation of the disk, which is much lower than the bandwidth required for basic tracking in a single-beam system. A low-bandwidth correction of q_T combined with a high-bandwidth servo on one of the beams in the array could completely correct tracking errors in a multiple-beam system.

The estimations of q_T in Figs. 1(b) and 2(b) give motivation for wavelength-domain tracking (WDT). WDT systems provide variation in beam separation as a function of disk radius, as well as individual control of beam positions. These advantages make simultaneous multitrack recording possible when combined with a high-bandwidth single-beam servo.

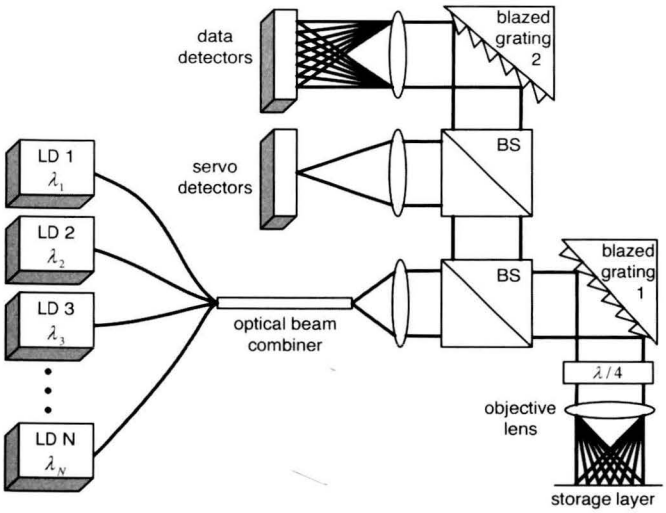

Fig. 3 Schematic of WDT system implementation.

The multitrack read/write enables WDT systems to transfer data faster than a single-beam optical storage system. The increase in the data transfer rate of WDT systems is nearly proportional to the number of laser sources used. However, the effective increase in the data rate is slightly reduced due to the dead time during track jumps, because the beam spot array should jump either multiple tracks or a single track repeatedly during one disk rotation to realize continuous parallel read/write operation using multiple beams.

This work is divided into several sections. Section 2 describes the basic concepts and system implementation of WDT. Also, mechanisms for tracking error detection and beam control in WDT systems are explained. Section 3 exhibits the experimental setup for a WDT feasibility test and its design specifications. Section 4 describes three experiments executed to prove the concept of WDT and provides experimental results. The conclusion and future work are presented in Sec. 5.

2 Principles of Wavelength-Domain Tracking

The main idea of WDT is to control the focused spot position of an individual beam by changing its wavelength. It exploits the dependence of diffraction angles on the wavelength of the light impinging on a grating. The wavelength change of the incident light gives rise to an angular change of the diffracted light. The resulting angular deviation repositions the focused beam spot on the recording surface. Likewise, when a multibeam light source with individual laser tunability is used, each individual beam illuminating adjacent tracks is controlled by tuning the wavelength of each laser. Therefore, beam spot separations are optimized to minimize q_T errors.

In the WDT system of Fig. 3, multiple beams with different wavelengths from separate emitters are merged into a single beam by means of an optical beam combiner, such as an optical fiber or optical waveguide. These wavelength-multiplexed beams follow the same optical path to wavelength-dispersive blazed grating 1. The beams are diffracted into different angles after reflection from blazed grating 1, where the multiplexing conversion from the wavelength domain to the angular domain takes place. Grating 1 and the objective lens distribute each individual component of the multiplexed beam onto separate tracks. The reflected beams from the medium are recombined into a single beam after the second reflection from grating 1. That is, the beams are remultiplexed in the wavelength domain. The wavelength multiplexed beam is then directed to servo and data detectors. Error signals for each channel are extracted by low-frequency modulation of individual lasers using a single servo detector and bandpass filters. For data readout, blazed grating 2 is used to distribute each reflected beam to individual data detectors. In case of q_T errors, laser wavelengths are tuned so that the beams follow the track centers. It is notable that blazed gratings, instead of simple diffraction gratings, are used due to their high diffraction efficiency into a specific order.

Tracking errors in WDT systems are sensed by a split-cell detector and extracted by multiple electronic bandpass filters. When a beam is reflected from the storage layer, phase differences between diffraction orders generate a pattern at the exit pupil that is called a "baseball pattern."[5] The baseball pattern has two overlapped areas, and the brightness of each overlapped area is determined by the relative position of the focused beam spot and the center of the nearest track. When the focused spot is centered on a track, the overlap areas are of equal brightness. As the spot moves away from the track center, the brightness of the overlap areas becomes unbalanced. The detection of unbalance in the baseball pattern gives rise to a tracking error signal (TES), which is explained more fully in Sec. 3. This baseball-pattern effect is observed for each wavelength independently.

Individual lasers are modulated at low frequencies (~100 kHz) with a separation of several kilohertz. The reflected beams after remultiplexing into the wavelength domain contain tracking error information (baseball patterns) for all the laser channels. A split-cell detector receives the combined beam, and separate bandpass filters sort out tracking error signals within a designated frequency range. Then, the extracted individual TES signals are fed back to servo electronics, and the amount of wavelength tuning is determined by feedback circuits. Thereafter, off-center beam spots are moved to track centers, and TES signals are kept to zero through the closed-loop feedback of the tracking servo. It should be pointed out that the low-frequency modulation of lasers does not affect data readout or focusing control, since a frequency separation of 100 kHz is allocated between data frequencies (~a few megahertz) and servo frequencies (~a few kilohertz).

Figure 4 illustrates the mechanism of controlling a single laser beam in the wavelength domain. A beam is diffracted at an angle $\Delta\theta_d$ from the blazed grating, and it is focused on the storage layer through an objective lens. Tuning of the laser wavelength by $\Delta\lambda$ gives rise to deviation of the diffracted angle by $\Delta\theta_d$. The angular deviation $\Delta\theta_d$ produces a lateral shift of the focused beam spot by Δx when multiplied by the objective lens focal length f. That is,

$$\Delta x = f\Delta\theta_d . \tag{13}$$

This lateral shift is possible because of telecentricity intro-

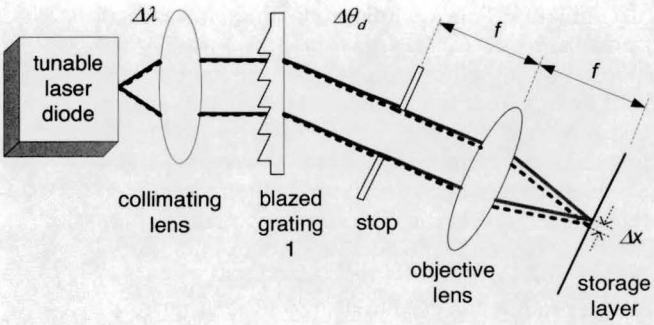

Fig. 4 Mechanism of controlling a single laser beam in the wavelength domain.

duced by placing the aperture stop at the front focal plane of the objective lens. The telecentric condition implies that the chief rays at the image plane are always perpendicular to the storage layer, regardless of angular deviation at the grating. Therefore, the reflected beam returns to the grating following the same path as the incident beam.

To find the relation between the amount of tuning $\Delta\lambda$ and lateral beam shift Δx, diffraction from a reflective blazed grating is examined. Diffraction is determined by the grating equation

$$p(\sin\theta_i+\sin\theta_d)=m\lambda, \tag{14}$$

where θ_i is the angle of the incident light, θ_d is the m'th-order diffraction angle, p is the period of the grating, and λ is the wavelength of the incident light. The differentiation of Eq. (14) with respect to diffraction angle and wavelength gives rise to the relation between tuning and angle deviation. That is,

$$\Delta\theta_d=\frac{m}{p\cos\theta_d}\Delta\lambda. \tag{15}$$

Using Eq. (15), the beam shift Δx is determined in terms of the objective lens focal length, the tuning amount, the grating pitch, and the diffraction angle. That is,

$$\Delta x=f\Delta\theta_d=\frac{mf}{p\cos\theta_d}\Delta\lambda. \tag{16}$$

The amount of tuning is also calculated for a given beam shift. That is,

$$\Delta\lambda=\frac{p\cos\theta_d}{mf}\Delta x. \tag{17}$$

The tuning amount $\Delta\lambda$ is proportional to the beam shift Δx.

3 Experimental Setup and Design

An experimental setup for testing the feasibility of WDT is shown in Fig. 5. An external cavity diode laser (ECDL) with a tuning range of 6 nm is used as a tunable laser source. The ECDL is fabricated by antireflection coating the front facet of a commercially available laser diode and placing a simple diffraction grating outside the diode to return the first diffraction order into the laser cavity. A simple grating with a period of 1 μm is holographically fabricated and coated with gold to provide reflection. The s-polarized zero-order output laser beam leaving the ECDL is directed to blazed grating 1 with a period of 10 μm and a blaze angle of 2.3 deg through various optics, and is turned by 90 deg on diffraction from the grating. Depolarization of the incident and reflected beams on the grating is expected to be negligible, since the grating period is considerably greater than the laser wavelength. The beam then passes through a quarter-wave plate and a stop. An objective lens with a focal length of 3.6 mm and a numerical aperture of 0.4 is used to focus the laser beam to a small spot on a fragment of an unwritten CD-R disk. A piezoelectric transducer (PZT) is used to produce tracking errors by moving the disk in the cross-track direction. When reflected, a baseball pattern is generated at the exit pupil of the system due to interference between diffracted orders. A split-cell detector is aligned such that each cell senses the light intensity of each half of the baseball pattern. A tracking error signal (TES) is determined by the difference of the two detector signals divided by their sum.[5] That is, the normalized TES is

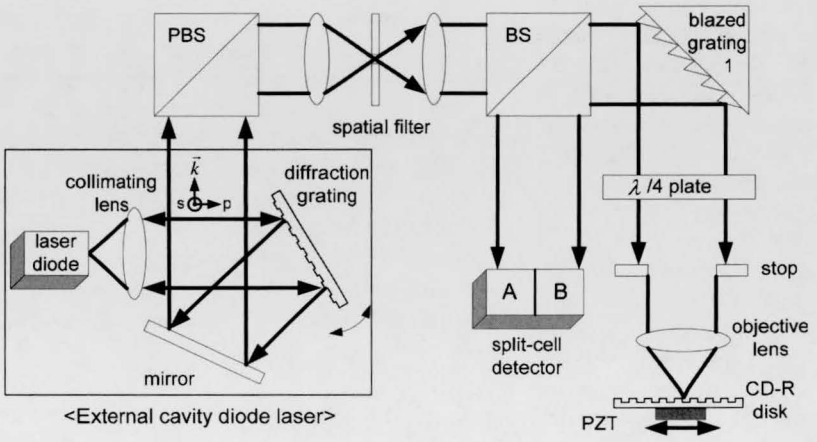

Fig. 5 Schematic of an experimental system for testing the feasibility of WDT.

$$\mathrm{TES}=\frac{A-B}{A+B}, \tag{18}$$

where A and B are the signals out of each detector cell. Notice that the experiment involves only one laser beam, and blazed grating 2, as shown in Fig. 3, is not implemented. Also, since only one laser beam is used, low-frequency laser modulation is not necessary to separate TES signals.

The amount of tuning needed for lateral beam shift is calculated as follows. The light impinging blazed grating 1 is set to be deflected by 90 deg into the first order, such that $\theta_d-\theta_i=90$ deg. After replacing the incident angle in Eq. (14) by $\theta_i=\theta_d-90$ deg and manipulating the equation using a trigonometric relation, the equation for the angle of the first-order diffracted beam is given by

$$\theta_d=45\ \deg+\sin^{-1}\left(\frac{\lambda}{p\sqrt{2}}\right). \tag{19}$$

From Eq. (19) and $\theta_d-\theta_i=90$ deg, the first-order diffraction angle and the incident angle are $\theta_d=47.6$ deg and $\theta_i=42.4$ deg, respectively. The amount of tuning for the lateral shift of the focused beam spot is calculated from Eq. (17) and $\theta_d=47.6$ deg. The tuning amounts for a half track ($\Delta x=0.8\ \mu$m) and one track ($\Delta x=1.6\ \mu$m) are 1.5 and 3 nm, respectively. For a beam crossing j tracks, the wavelength needs to be tuned by j times 3 nm.

In the design of a WDT system, spurious optical feedback should be taken into consideration, since performance of a WDT system depends on spectral behaviors of tunable lasers. Sensitivity to optical feedback is tested with two types of tunable laser sources, which are a thermally controlled tunable laser and an ECDL. When a WDT system is implemented with a thermally controlled laser diode, it is observed that the lasing wavelength jumps among a few longitudinal modes, and that the dominant mode wavelength is a function of the beam position on the disk. This problem of modehopping is solved by use of an ECDL as a tunable laser source. The diffraction grating used in an ECDL plays a major role in reducing the spurious feedback noise, due to its wavelength-filtering ability. Therefore, the ECDL is a good candidate for a tunable laser source of a WDT system in the aspect of feedback suppression.

4 Experiment and Result

The concept of WDT is proven by demonstrating that wavelength tuning causes a focused beam spot to move a designed distance on a storage layer. In the first experiment, a simulated TES signal and an experimentally obtained TES signal are compared. In the second experiment, the phase shift of a TES signal due to wavelength tuning is observed when the disk position is modulated by a PZT in the cross-track direction. In a third experiment, a digital tracking servo for WDT systems is developed and demonstrated.

For the first experiment, baseball patterns and the resulting TES signals are simulated as a function of spot position on the disk. The simulation is based on an optical system with a Geltech lens (350022) as an objective lens and a fraction of CD-R disk as a target. The information on the light between the objective lens and the disk is obtained using ZEMAX (ZEMAX Development Corporation) and transferred to OPTISCAN,[6] a physical optics simulation tool, for the calculation of light propagation, interference patterns at the exit pupil, and light intensities at the detector cells. As the focused spot on the storage layer in Fig. 6 is moved in the cross-track direction by steps of 0.2 μm for a total distance of one track, nine baseball patterns are obtained and shown in Fig. 7. The numbers in Figs. 6 and 7 represent locations of the focused beam spot on the storage layer. It is observed that the two overlapped areas are of equal brightness when the focused beam is centered on a groove (position 3) or land (position 7) and become unbalanced when the beam spot moves away from the center, which is as expected.[7] The resultant normalized TES signal, as shown in Fig. 8, has a sinusoidal waveform with a period corresponding to the track pitch.

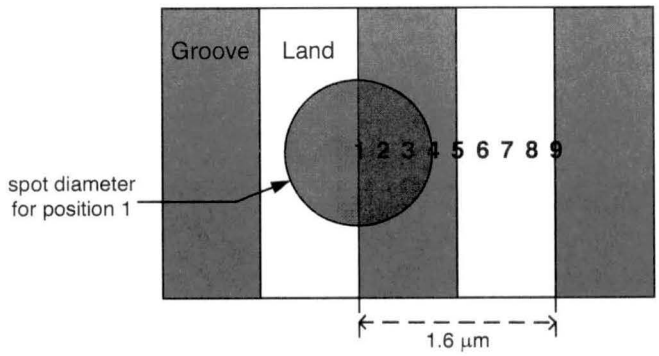

Fig. 6 A small fragment of a CD-R storage layer. The numbers correspond to the possible positions where the focused beam illuminates the tracks. Adjacent positions are separated by 0.2 μm.

Baseball patterns are also obtained from two separate configurations: one by disk translation and the other by focused spot translation due to wavelength tuning. For the former configuration, the disk is moved by steps of 0.4 μm for a total length of one track by use of a PZT. In the latter configuration, the laser wavelength is tuned by 2.93 nm so that the focused beam moves across a total distance of one track, which is the same total distance as with PZT-controlled disk movement. Photographs of the baseball patterns captured on a CCD camera in the two configurations

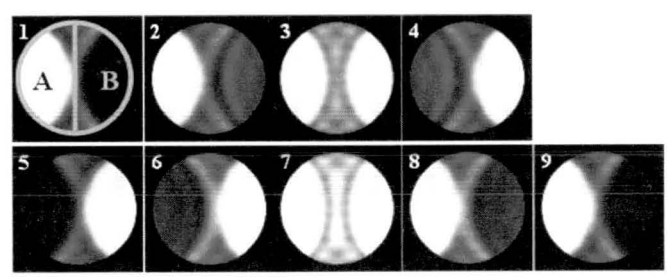

Fig. 7 Simulated baseball patterns with a beam spot illuminating different positions of a track. The first baseball pattern is generated from a beam illuminating spot position 1 in Fig. 6. Then, the disk is translated by 0.2 μm to the left, so that the next baseball pattern comes from beam position 2. The ninth baseball pattern is the same as the first one, since both beams illuminate a land/groove border.

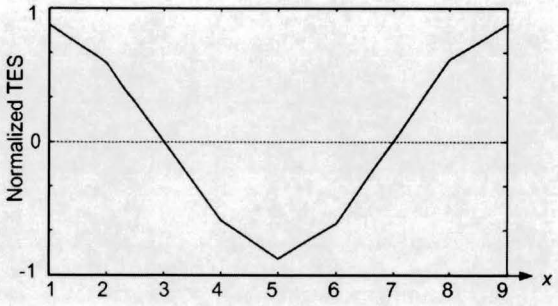

Fig. 8 TES signal calculated when the baseball patterns in Fig. 6 illuminate a split-cell detector.

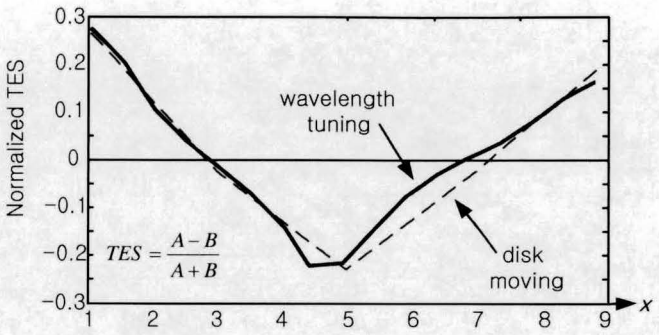

Fig. 10 Comparison of experimentally obtained TES signals obtained by wavelength tuning and by disk translation.

are shown in Figs. 9(a) and 9(b). The numbers correspond to the spot positions in Fig. 6. The baseball patterns for each position from the two configurations look alike, as expected. For a more exact comparison, TES signals are calculated by image processing the pictures of the baseball patterns in Fig. 9. To calculate the TES signal from the images, the pixel intensities on the left and the right halves of the images are summed separately. Their subtraction and division by their sum result in a normalized TES given by Eq. (18). Following this procedure, the TES signal levels for the baseball pattern images in Figs. 6(a) and 6(b) are calculated, and the resulting TES curves are shown in Fig. 8. Due to the equivalent effects of moving the disk and tuning the wavelength in WDT systems, the TES signals from the two configurations are expected to match up. As seen in Fig. 10, the two experimentally obtained TES signals are in good agreement. Also, they are in accordance with the simulated TES signal in Fig. 8.

The second experiment shows that a beam moves a designed distance by measuring phase shifts caused by wavelength tuning. Tuning-caused phase shift of a TES signal in the experimental WDT system is observed when the disk is modulated at a frequency of 1 Hz in the cross-track direction using a PZT. The disk modulation makes the focused beam scan over several tracks and generates a sinusoidal TES signal. If the focused beam spot is displaced from the original location by wavelength tuning, the phase of the TES signal changes. For example, if the focused beam spot moves from a land center to a groove center by changing the wavelength of the laser, the TES signal changes phase by π radians. If it moves across one track, then a phase shift of 2π is observed. Figure 11 shows the initial TES signal before wavelength tuning and two phase-shifted TES signals with tuning increments of $\Delta\lambda = 1.5$ nm and $\Delta\lambda = 3$ nm. These increments are calculated in Sec. 4 for the purpose of moving the focused spot by half a track and one track, respectively. Figure 11 shows that, as expected, a tuning of $\Delta\lambda = 1.5$ nm causes the phase of the initial TES signal to shift by π. The TES signal obtained by tuning of $\Delta\lambda = 3$ nm overlaps with the initial TES signal. Therefore, observation of the expected phase shift in a TES signal suggests that the focused beam moves the designed distance across the track.

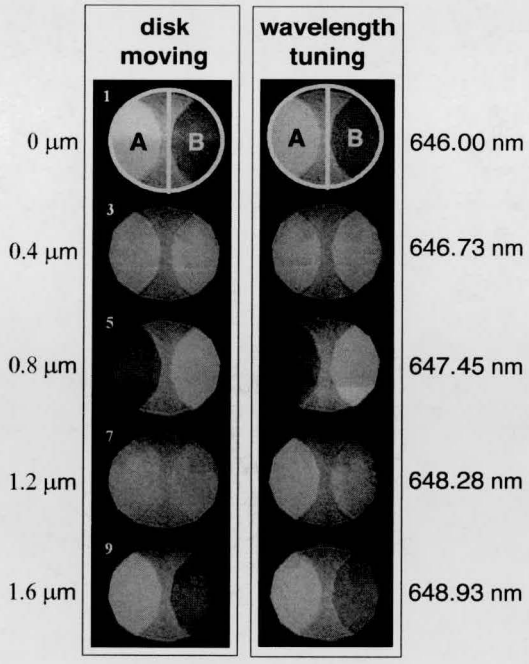

Fig. 9 Photographs of baseball patterns captured on a CCD camera. (a) Baseball patterns obtained by moving the disk by steps of 0.4 μm. (b) Baseball patterns obtained by wavelength tuning. The laser wavelength is tuned to move the focused beam spot for a total distance of one track. The increment of the wavelength tuning is about 0.75 nm, and the total tuning range is about 2.93 nm.

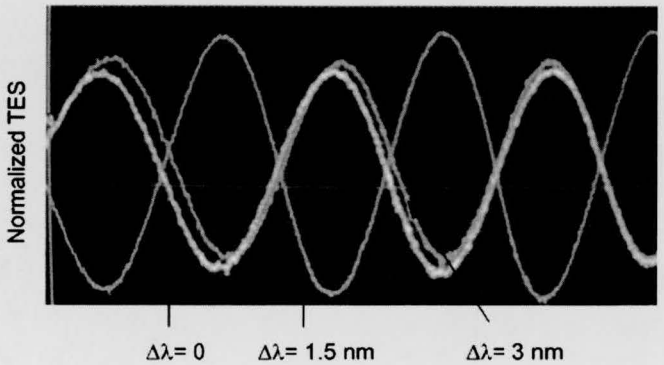

Fig. 11 TES signal traces at different wavelengths. Phase shifts of π and 2π are observed for beam crossing of half a track and one track, when the disk is modulated at a frequency of 1 Hz in the cross-track direction using a PZT.

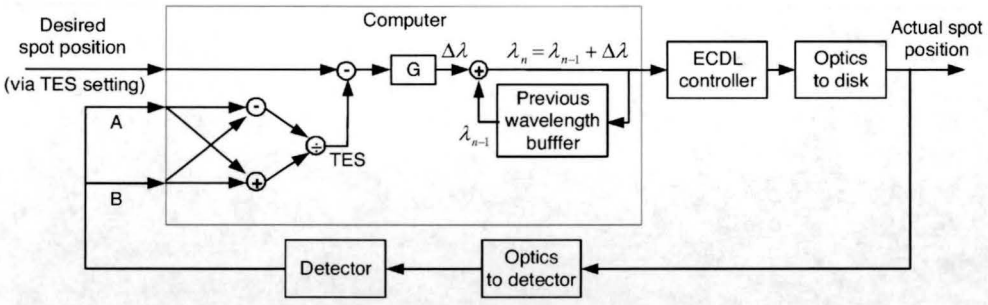

Fig. 12 Closed-loop control system for a WDT servo.

Finally, a digital tracking servo for WDT systems is developed in the third experiment using a computer and a commercial ECDL (Newfocus, Incorporated) with center wavelength 672 nm and a minimum tuning range of 12 nm. The lasing wavelength of the ECDL is determined by the closed-loop control system shown in Fig. 12. The information on the desired spot position via the desired TES setting is sent to the computer. The actual TES is calculated in the computer, based on Eq. (18). Then, the amount of wavelength tuning $\Delta\lambda$ is determined by multiplication of the tracking error value and a feedback gain G. The computer sends to the ECDL controller a command for a modified wavelength λ_n, which is calculated by a sum of the wavelength λ_{n-1} in the previous loop and the amount of required wavelength tuning. The tuned wavelength moves the focused spot toward the track center.

Figure 13 shows the layout of a WDT tracking servo with the closed-loop control system. The ECDL output beam is focused on a disk and reflected from it. The reflected beam that contains a baseball pattern is directed to a split-cell detector. Then, the two detector signals are sent to the computer. The required wavelength is calculated in the computer from the detector signals after digitization and sent to the ECDL controller to tune the laser wavelength. By repeating this procedure in a closed-feedback loop, the tracking errors caused by beam displacement from the desired position are minimized.

In the WDT servo shown in Fig. 13, tracking errors are generated by modulating the disk position with a PZT at a frequency of 0.05 Hz in the cross-track direction. The TES signal is simultaneously calculated from the digitized detector signals. Figure 14 shows the TES signal with the servo on and off. While the servo is off, the TES signal has a sinusoidal waveform, which is in good agreement with the simulated and experimental results. When the servo is activated, the sinusoidal TES signal drops nearly to zero. The ECDL tunes the lasing wavelength by the appropriate amount in the closed-loop feedback system. Figure 14 demonstrates the feasibility of WDT systems. However, tracking speed in this experiment is limited by the tuning speed of the ECDL. The ECDL uses a PZT for fine tuning ($<$0.01 nm) and a motor for coarse tuning ($>$0.01 nm). To keep the focused beam spot on track center, the ECDL needs to move the simple grating forward and backward frequently using the motor, since the required wavelength tuning is greater than 0.01 nm in this experiment. When the wavelength needs to be tuned more frequently than the motor settling time allows, the ECDL output beam generates a false TES signal. Therefore, a slow speed was used. Other

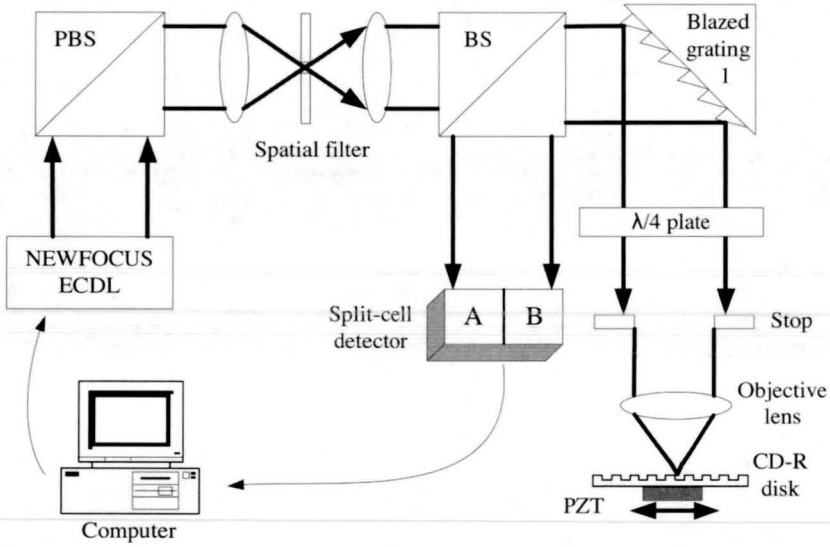

Fig. 13 Layout of a digital tracking servo for a WDT system.

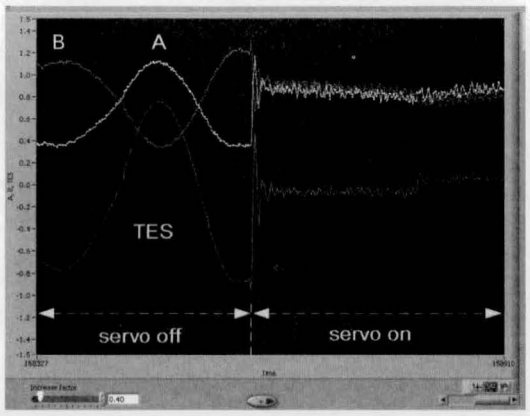

Fig. 14 TES signal with the WDT tracking servo off and on. The sinusoidal TES signal decreases significantly when the tracking servo is activated.

wavelength-tuning systems show faster response,[8] but they could not be incorporated into this experiment.

5 Conclusion

A wavelength-domain tracking system is developed and demonstrated for multibeam optical storage. With its capability to individually control beam positions, a WDT system can overcome problems in controlling beam spot spacing as a function of disk radius and disk decenter, which is a problem that all multibeam optical storage systems have. Also, a novel method of error signal extraction by low-frequency modulation is proposed.

The feasibility of a WDT scheme is tested in the following three ways. First, baseball patterns and TES signals from simulation and two configurations are compared, and the match-up of the results demonstrates that track following of a beam is possible in the wavelength domain. Second, the phase shift of a TES due to wavelength tuning is observed when the disk is modulated in the cross-track direction by a PZT. The observation of the expected tuning-caused phase shift in the TES indicates that wavelength tuning causes the focused beam to move by the designed distance. Finally, a digital tracking servo for WDT systems is developed and demonstrated. Activating the closed-loop servo flattens a sinusoidal TES, and locking a beam on a track center is achieved.

For future work, a WDT system needs to be implemented using multiple tunable laser sources and an optical beam combiner. Also, improvement in wavelength-tuning characteristics of tunable laser sources, such as tuning speed, is necessary. Feedback tolerance needs to be considered in the selection of tunable laser sources for a WDT system, and ECDL sources appear to be attractive devices for this purpose.

Acknowledgment

This work is supported by contract (NAS2-00117) from the National Aeronautics and Space Administration. We thank Yan Zhang, John Butz, and Warren Bletscher for valuable discussions.

References

1. A. Alon and T. Kosoburd, "Multi-beam optical pickup," U.S. Patent No. 6,411,573 (2002).
2. R. Katayama, K. Yoshihara, Y. Yamanaka, M. Tsunekane, K. Kayanuma, T. Iwanaga, O. Okada, and Y. Ono, "Multi-beam optical disk drive for high data transfer rate systems," *Jpn. J. Appl. Phys., Part 1* **31**(2B), 630–634 (1992).
3. H. Okumura, K. Arai, N. Kawamura, H. Tokumaru, and H. Okuda, "Multi-beam light source using optical waveguide for optical recording," *Proc. SPIE* **4090**, 329–334 (2000).
4. K. Sasaki, D. Koide, H. Yanagisawa, H. Tokumaru, and Y. Fujita, "Blue-violet 2-beam optical head for high-speed recording," *Tech. Dig. Opt. Data Storage 2003*, pp. 155–157 (2003).
5. T. D. Milster, "Optical data storage," in *The Optics Encyclopedia: Basic Foundations and Practical Applications*, T. G. Brown, K. Creath, H. Kogelnik, M. A. Kriss, J. Schmit, and M. J. Weber, Eds., Wiley-VCH, Germany (2004).
6. T. D. Milster, "Physical optics simulation in Matlab for high-performance systems," *Opt. Rev.* **10**, 246–250 (2003).
7. A. B. Marchant, *Optical Recording: A Technical Overview*, Addison-Wesley, Reading, MA (1990).
8. J. D. Berger, D. Anthon, and H. Jerman, "External cavity diode lasers tuned with silicon MEMS," *Semiconductor Intl.* **25**(2), 8–14 (2002).

Taeyoung Choi received his BS degree in radio communication engineering from Yonsei University Korea (2001) and MS in electrical engineering from University of Arizona (2004). He is currently pursuing his PhD degree in optical sciences at the University of Arizona. His current research interests include servo techniques in optical data storage and erasure of data written on writable optical disks. He is a member of SPIE.

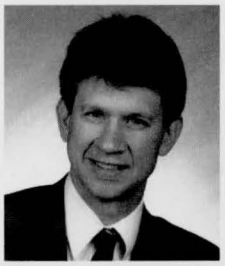

Tom D. Milster received his BS in electrical engineering from the University of Missouri-Rolla in 1981, and his PhD in optical sciences from the University of Arizona in 1987. He started his career as an optical engineer with IBM Corporation in 1986, where he worked on advanced technologies for optical data storage. He joined the University of Arizona faculty in 1989, and is now a research professor of optical sciences at the Optical Sciences Center. His major research interest is the study of physical optics phenomena in high-performance optical systems. In particular, a large part of his research involves microscopy and optical data storage, which includes high-density near-field scanning, volumetric storage, data detection, and servo techniques. He is also involved with lithography research. An extreme ultraviolet spectrometer designed by him was part of the scientific package that recently flew in the space shuttle with Senator John Glenn. He is a Fellow of the Optical Society of America and SPIE.

Matthew Lang: Biography and photograph not available.